Science Advances
AAAS

Supplementary Materials for

Activation of NOD1 on tumor-associated macrophages augments $CD8^+$ T cell–mediated antitumor immunity in hepatocellular carcinoma

Feng Zhang *et al.*

Corresponding author: Si Zhang, zhangsi@fudan.edu.cn; Ling Dong, dong.ling@zs-hospital.sh.cn; Ruyi Xue, xue.ruyi@zs-hospital.sh.cn

Sci. Adv. **10**, eadp8266 (2024)
DOI: 10.1126/sciadv.adp8266

This PDF file includes:

Fig. S1

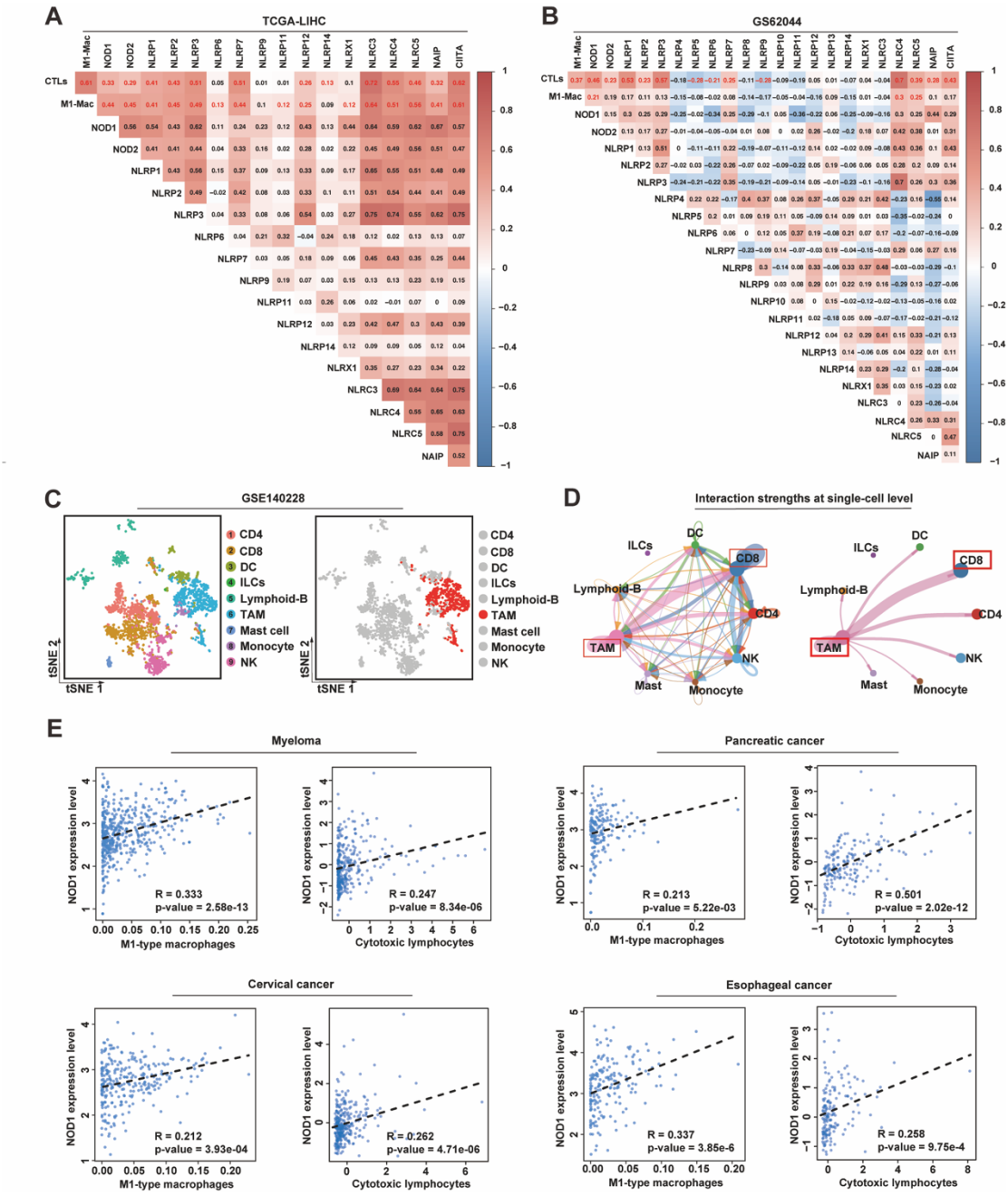

Fig. S1. Integrated transcriptome analyses unveil the involvement of NOD1 in anti-tumor immunity. (A-B) Heatmaps displaying spearman correlations among NLRs, M1-type macrophages, and CTLs in HCC patients from the TCGA-LIHC (A) and GEO (GSE62044) (B) datasets. (C-D) Single-cell analysis of tumor samples from HCC patients (GSE140228). tSNE plot illustrating distinct cell subsets (A, left panel), with the TAM population highlighted in red (A, right panel).

Cell-cell communication network identified by CellChat, where nodes represent cell types and edges represent ligand-receptor interaction strength (B). (E) Scatterplot results from the spearman correlation analysis of NOD1 expressions with M1-type macrophages or CTL infiltrations across diverse cancer patients. HCC: hepatocellular carcinoma; tSNE: t-Distributed Stochastic Neighbor Embedding; TAM: tumor-associated macrophage; NLRs: NOD-like receptors; CTLs: cytotoxic T lymphocytes; TCGA-LIHC: The Cancer Genome Atlas Liver Hepatocellular Carcinoma; GEO: Gene Expression Omnibus; DC: dendritic cell; ILC: innate lymphoid cell; NK: natural killer.

Fig. S2

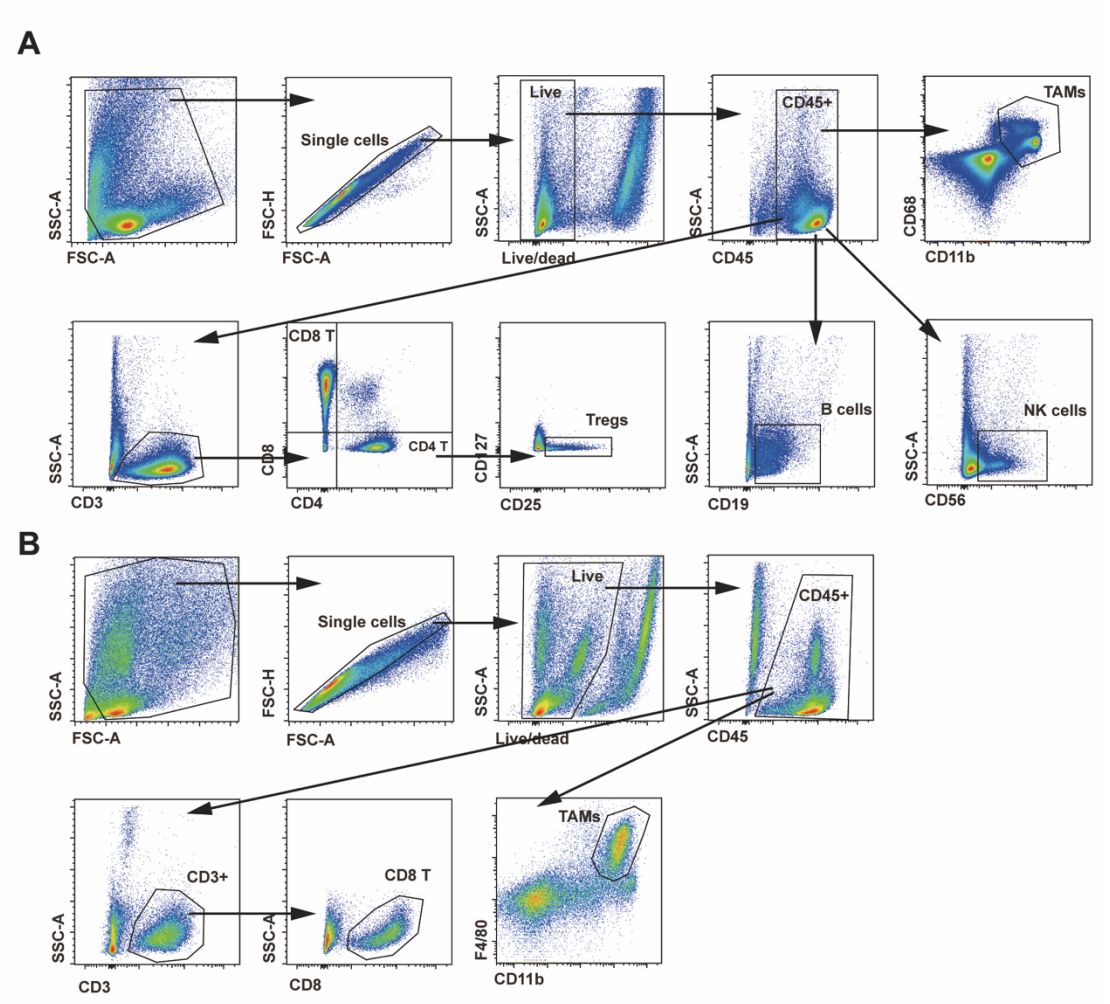

Fig. S2. Gating strategies used for cell sorting and flow cytometric analysis. (A) Gating strategy for analyzing TAMs, $CD8^+$ T-cells, Tregs, B cells and NK cells in tumor samples from HCC patients. (B) Gating strategy for analyzing TAMs and $CD8^+$ T-cells in murine tumor samples. TAM: tumor-associated macrophage; NK: natural killer; SSC-A: side scatter area; FSC-A: forward scatter area; FSC-H: forward scatter height.

Fig. S3

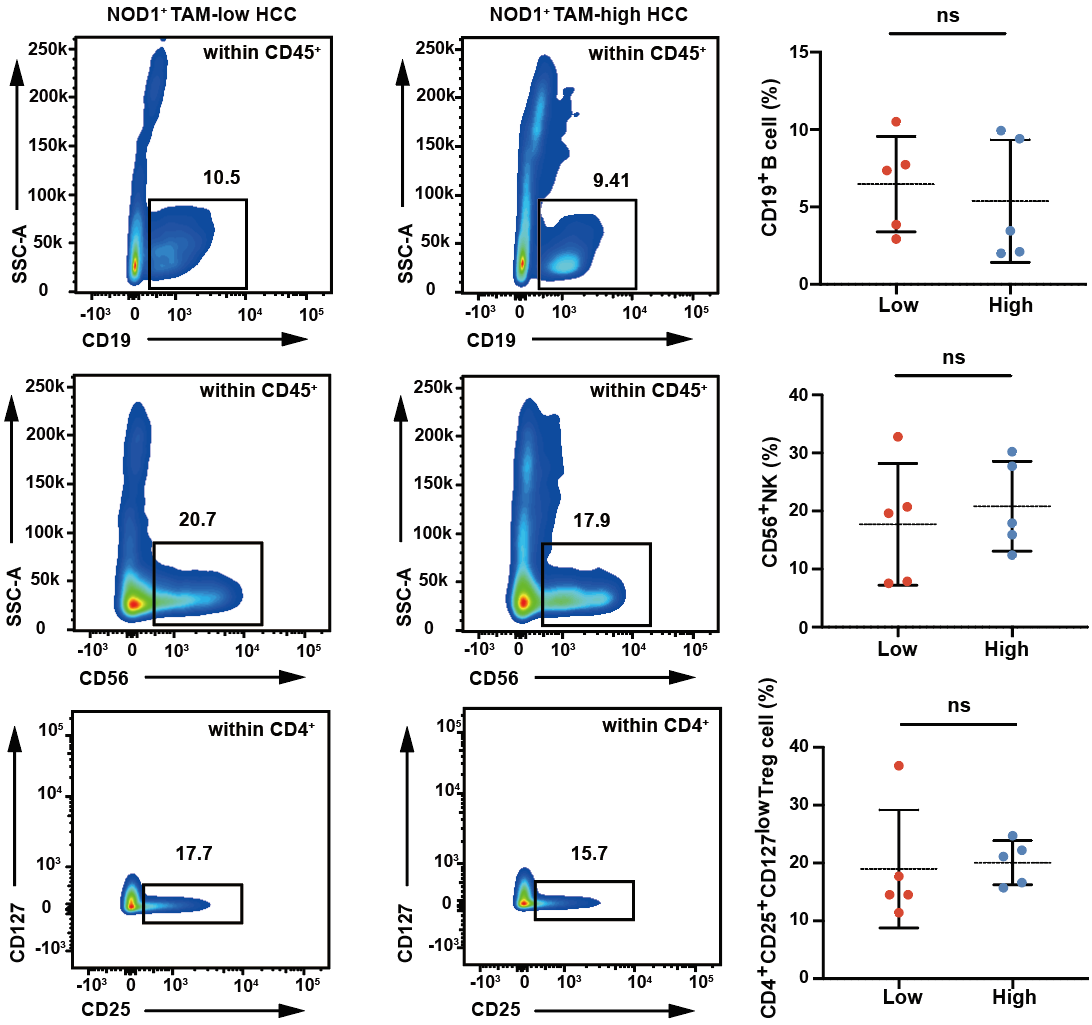

Fig. S3. Flow cytometric analysis of B cells, NK cells, and Tregs in human HCC samples. The proportions of $CD19^+$ B cells, $CD56^+$ NK cells, and $CD4^+$ $CD25^+$ $CD127^{low}$ Tregs were compared in HCC samples with low- and high-$NOD1^+$ TAMs (n=10). Statistical analysis was performed using the Student's t-test. Data was presented as mean with SD. ns, no significance. HCC: hepatocellular carcinoma; NK: natural killer; TAM: tumor-associated macrophage; SSC-A: side scatter area; SD: standard deviation.

Fig. S4

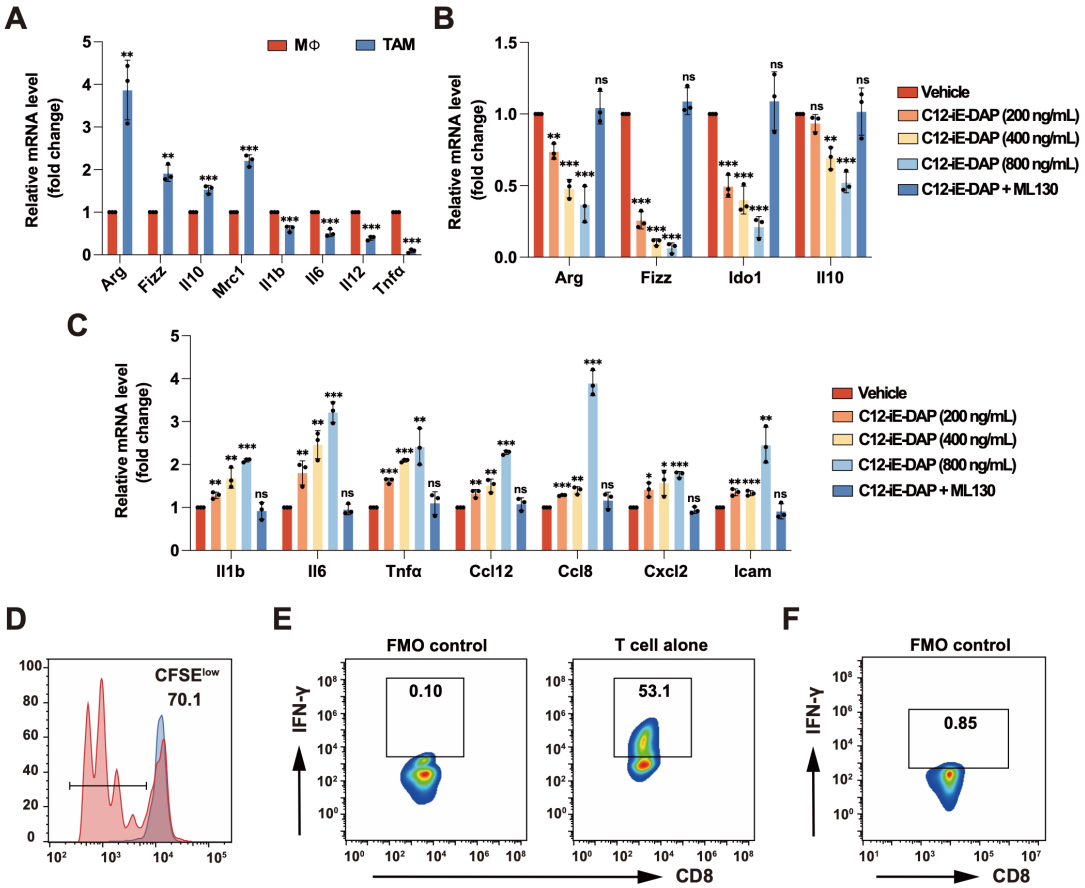

Fig. S4. NOD1 activation induces TAMs to acquire an immunostimulatory phenotype. (A) qPCR analysis of the mRNA levels of immune-regulatory genes in MΦ (untreated BMDMs) versus TAMs (TCM-educated BMDMs). (B) mRNA levels of immune-suppressive genes in TAMs treated with either C12-iE-DAP, C12-iE-DAP + ML130, or vehicle. (C) mRNA levels of immune-stimulatory genes in TAMs treated with either C12-iE-DAP, C12-iE-DAP + ML130, or vehicle. (D) Positive control for the T-cell proliferation assay. The percentage of CFSE low population for CD3/CD28 stimulated $CD8^+$ T cells without BMDMs is shown. (E) FMO control (left panel) and positive control (CD3/CD28 stimulated $CD8^+$ T cells alone, right panel) for flow cytometry analysis of co-cultured IFN-γ^+ $CD8^+$ T cells. (F) FMO control for flow cytometry analysis of co-cultured IFN-γ^+ OT-I $CD8^+$ T cells. Statistical analysis was performed using the Student's t-test. Data was

presented as mean with SD. ns, no significance; *p<0.05, **p<0.01, ***p<0.001 (vs. vehicle). TAM: tumor-associated macrophage; TCM: tumor condition medium; BMDM: bone marrow-derived macrophage; CFSE: carboxyfluorescein succinimidyl ester; FMO: fluorescence minus one; IFN-γ: interferon-γ; SD: standard deviation.

Fig. S5

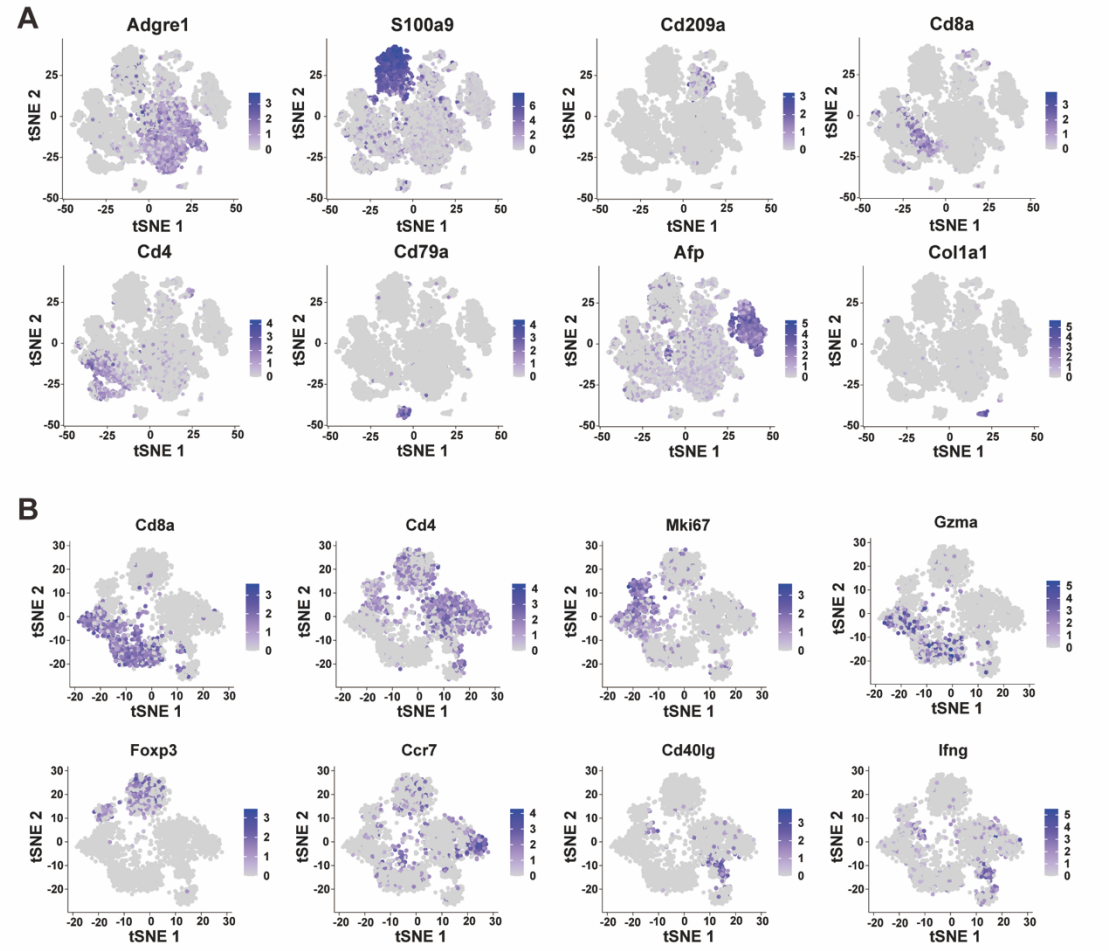

C

NO.	Cell Population	Signature genes
0	Mki67 high CD8 T cell	Mki67, Top2a, Stmn1
1	Foxp3 high Treg	Foxp3, Ctla4, Ikzf2, Icos, Tnfrsf4, Il2ra,Il10
2	Effector CD8 T cell	Gzmb, Gzma, CD8a, CD8b1, Ccl5
3	Icos high CD4 T cell	Icos, Cd4, Pdcd1
4	Ccr7 high naïve CD4 T cell	Ccr7, Tnfrsf4, Ramp3
5	T helper cell	Ifng, Cd40lg, Il2, Il4, Il21, Tnfsf11
6	Ifit1 high NKT cell	Ifit1, Ly6c2, Fosb, Klf2, Hspa1a, Hspa1b

Fig. S5. The scRNA-seq analysis of murine orthotopic HCC treated with either vehicle or C12-iE-DAP. (A) tSNE plots showing the expression of cell markers for $CD45^{+}$ cells. (B) tSNE plots showing the expression of cell markers for T-cells. (C) Signature genes of identified clusters of T-cells. scRNA-seq: single-cell RNA sequencing; HCC: hepatocellular carcinoma; tSNE: t-Distributed Stochastic Neighbor Embedding.

Fig. S6

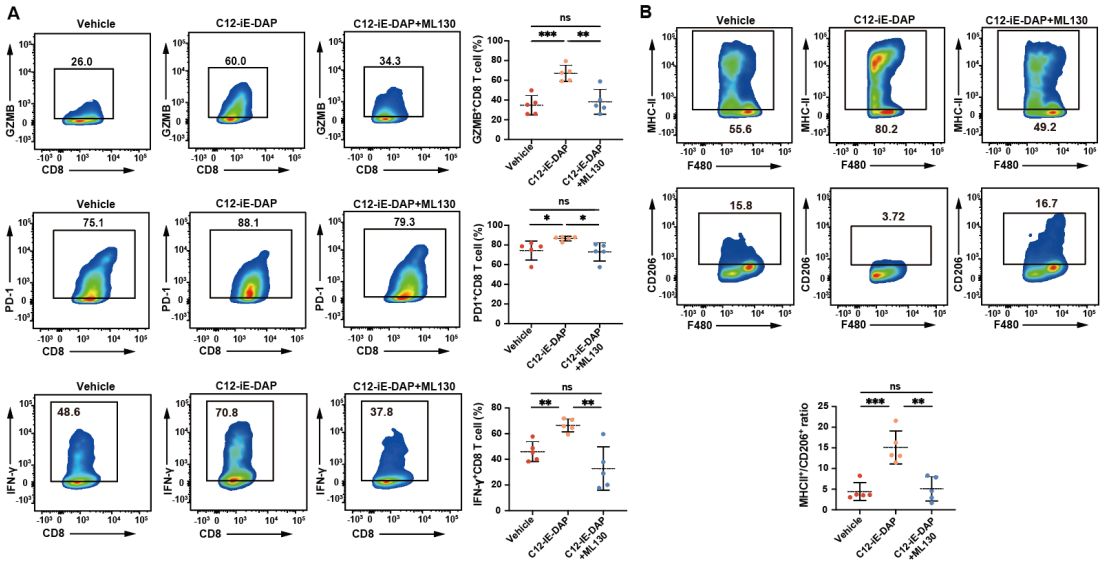

Fig. S6. Flow cytometric analysis of orthotopic HCC tumors treated with either C12-iE-DAP, C12-iE-DAP + ML130, or vehicle. (A) The representative data and statistical diagram of the percentages of $GZMB^+$, $PD\text{-}1^+$ or $IFN\text{-}\gamma^+$ $CD8^+$ T-cells are shown (n=5 each). (B) The representative data and statistical diagram of the MHC II: CD206 positive rates ratios of macrophages are shown (n=5 each). Statistical analysis was performed using the Student's t-test. Data was presented as mean with SD. ns, no significance; *p<0.05, **p<0.01, ***p<0.001. HCC: hepatocellular carcinoma; GZMB: granzyme B; SD: standard deviation.

Fig. S7

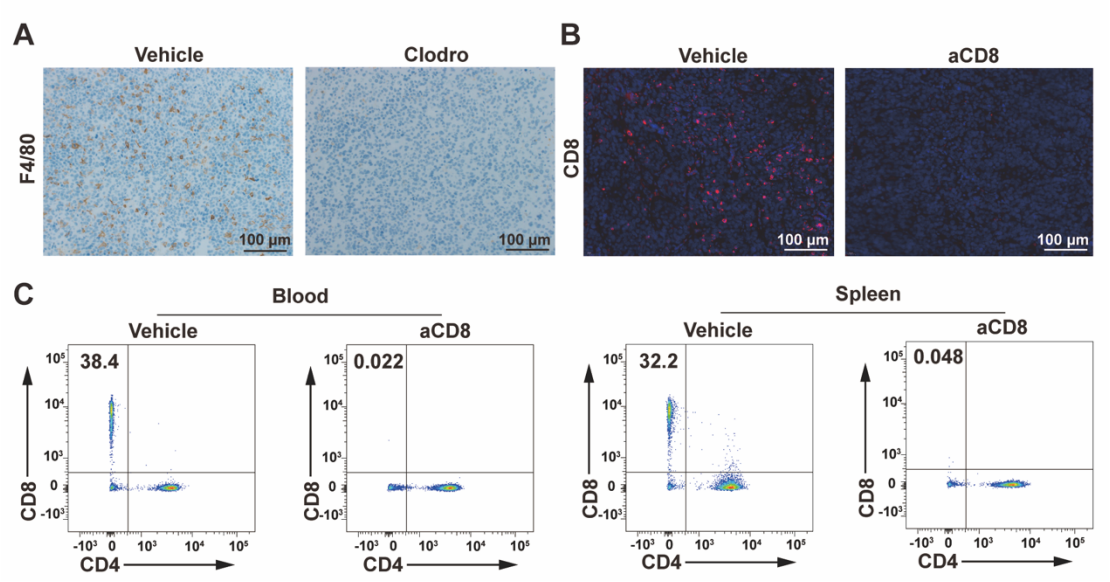

Fig. S7. Validation of the in vivo depletion efficiency of Clodronate Liposome and anti-mouse CD8α antibody. (A) Representative IHC images of F4/80^{+} macrophages in Hepa 1-6 tumors treated with either vehicle or Clodronate Liposomes. Scale bar: 100 μm. (B) Representative IF images of CD8^{+} T-cells in Hepa 1-6 tumors treated with either vehicle or depleting anti-CD8 antibody. Scale bar: 100 μm. (C) Flow cytometric analysis of blood (left panel) and spleens (right panel) from C57BL/6 mice treated with either vehicle or depleting anti-CD8 antibody. The proportions of CD8^{+} T-cells are shown. IHC: immunohistochemistry; IF: immunofluorescence.

Fig. S8

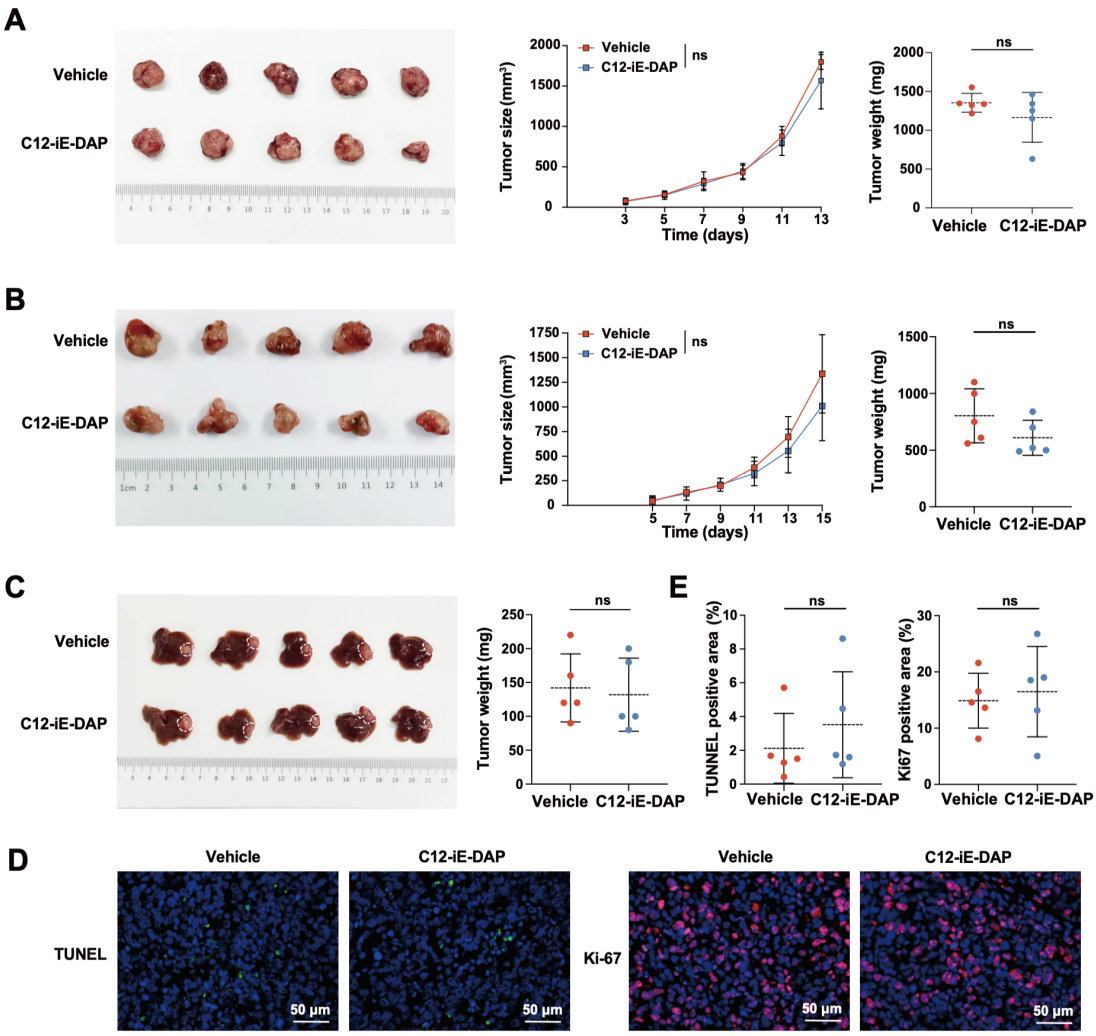

Fig. S8. Effect of the NOD1 agonist, C12-iE-DAP on tumor growth in immune-deficient SCID or BALB/c nude mice. (A) Tumor growth curves and tumor weights of HCC tumors from SCID mice treated intraperitoneally with either vehicle or C12-iE-DAP (25 μg/injection, every other day, n=5 each). (B) Tumor growth curves and tumor weights of BALB/c nude mice inoculated subcutaneously with Hepa 1- 6 cells, treated with either vehicle or C12-iE-DAP (n=5 each). (C) Representative pictures (left panel) and tumor weights (right panel) of orthotopic HCC of BALB/c nude mice inoculated with Hepa 1-6 cells, treated with either vehicle or C12-iE-DAP (n=5 each). (D-E) Representative pictures (D) and statistical diagrams (E) depicting the immunofluorescence

staining of TUNEL and Ki67 in orthotopic HCC treated with either vehicle or C12-iE-DAP (n=5 each). Scale bar: 50 μm. Statistical analysis was performed using the Student's t-test. Data was presented as mean with SD. ns, no significance. SCID: severe combined immunodeficiency; HCC: hepatocellular carcinoma; SD: standard deviation.

Fig. S9

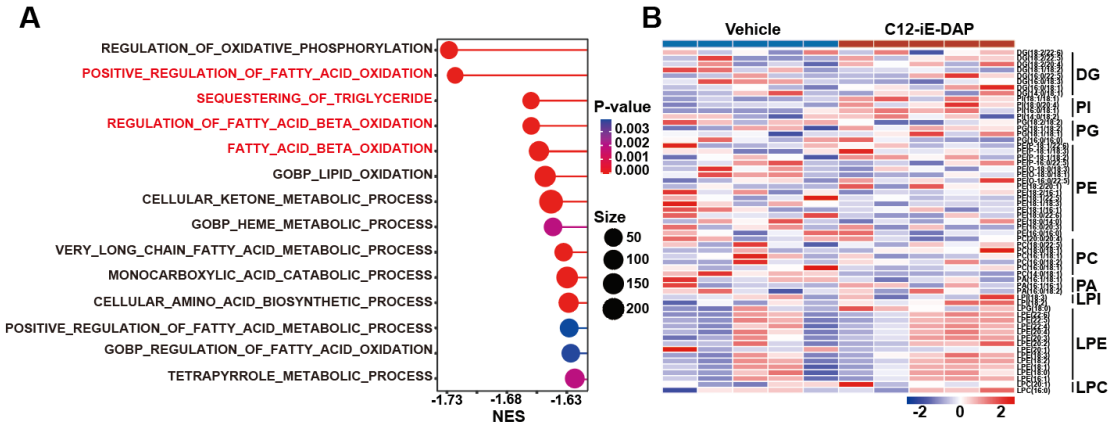

Fig. S9. NOD1 activation regulates fatty acid metabolism in TAMs. (A) GSEA enrichment analysis of NOD1$^+$ TAMs using scRNA-seq data from HCC patients (GSE140228). NOD1$^+$ TAMs were stratified into either NOD1-low or NOD1-high TAMs based on the median value of NOD1 expression. (B) Metabolomics analysis of diacylglycerol and major structural lipids in TAMs treated with either vehicle or C12-iE-DAP (400 ng/ml) for 24 h. TAM: tumor-associated macrophage; GSEA: Gene Set Enrichment Analysis; scRNA-seq: single-cell RNA sequencing; HCC: hepatocellular carcinoma; DG: diacylglycerol; PI: phosphatidylinositol; PG: phosphatidylglycerol; PE: phosphatidylethanolamine; PC: phosphatidylcholine; PA: phosphatidic acid; LPI: lysophosphatidylinositol; LPE: lysophosphatidylethanolamine; LPC: lysophosphatidylcholine; NES: Normalized Enrichment Score.

Fig. S10

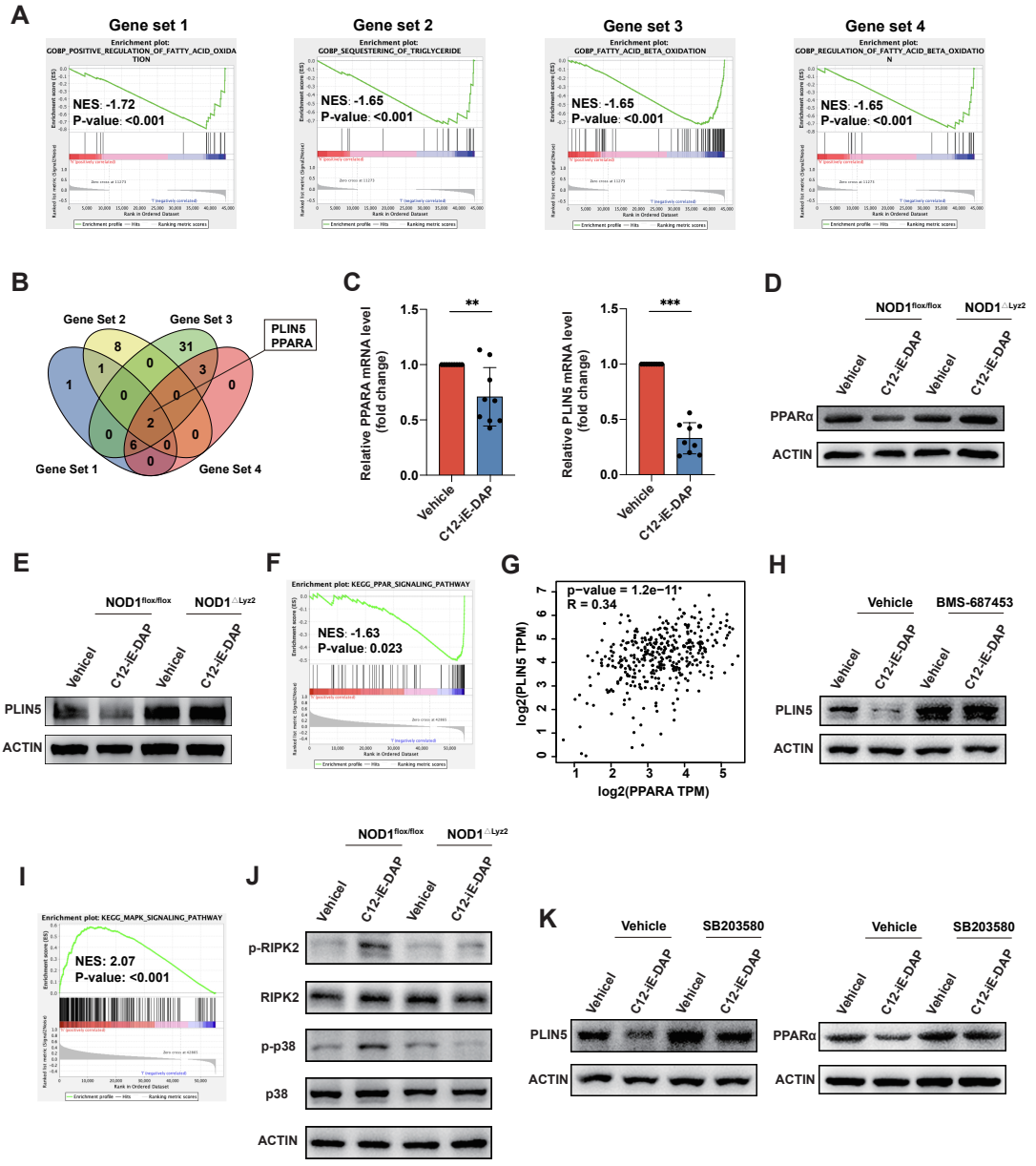

Fig. S10. NOD1 activation decreases PLIN5 expression by p38/PPARα pathway in TAMs. (A) GSEA plots of the top four differential lipid metabolism-related pathways between NOD1-low and NOD1-high TAMs in HCC (GSE140228). (B) Venn diagram showing the intersection of gene sets involved in the top four pathways enriched for lipid metabolism. (C) qPCR analysis of the mRNA levels of *PPARA* (left panel) and *PLIN5* (right panel) in TAMs treated with either vehicle or C12-iE-DAP (400 ng/ml) for 24 h. (D-E) The protein levels of PPARα (D) and PLIN5 (E) in TAMs that

were generated from NOD1$^{flox/flox}$ or NOD1$^{\Delta Lyz2}$ mice and treated with either vehicle or C12-iE-DAP (400 ng/ml). (F) GSEA analysis of TCGA-LIHC demonstrates the downregulation of PPAR signaling pathway in NOD1-high HCC compared to NOD1-low HCC. (G) Spearman correlation analysis of *PPARA* and *PLIN5* expressions using TCGA-LIHC. (H) The protein levels of PLIN5 in TAMs that pre-treated with vehicle or PPARα agonist (BMS-687453, 500 nM) for 12 h, and then treated with either vehicle or C12-iE-DAP (400 ng/ml) for 24 h. (I) GSEA analysis of TCGA-LIHC demonstrates the upregulation of MAPK signaling pathway in NOD1-high HCC compared to NOD1-low HCC. (J) The protein levels of p38, phosphorylated p38, RIPK2 and phosphorylated RIPK2 in TAMs that were generated from NOD1$^{flox/flox}$ or NOD1$^{\Delta Lyz2}$ mice and treated with either vehicle or C12-iE-DAP (400 ng/ml). (K) The protein levels of PPARα (left panel) and PLIN5 (right panel) in TAMs that pre-treated with vehicle or p38 inhibitor (SB203580, 10 μM) for 12 h, and then treated with either vehicle or C12-iE-DAP (400 ng/ml) for 24 h. Statistical analysis was performed using the Student's t-test. Data was presented as mean with SD. ns, no significance; **p<0.01, ***p<0.001. PLIN5: perilipin 5; PPARα: Peroxisome Proliferator-Activated Receptor α; GSEA: Gene Set Enrichment Analysis; TAM: tumor-associated macrophage; HCC: hepatocellular carcinoma; TCGA-LIHC: The Cancer Genome Atlas Liver Hepatocellular Carcinoma; MAPK: Mitogen-Activated Protein Kinase; RIPK2: Receptor-Interacting Protein Kinase 2; SD: standard deviation; NES: Normalized Enrichment Score.

Fig. S11

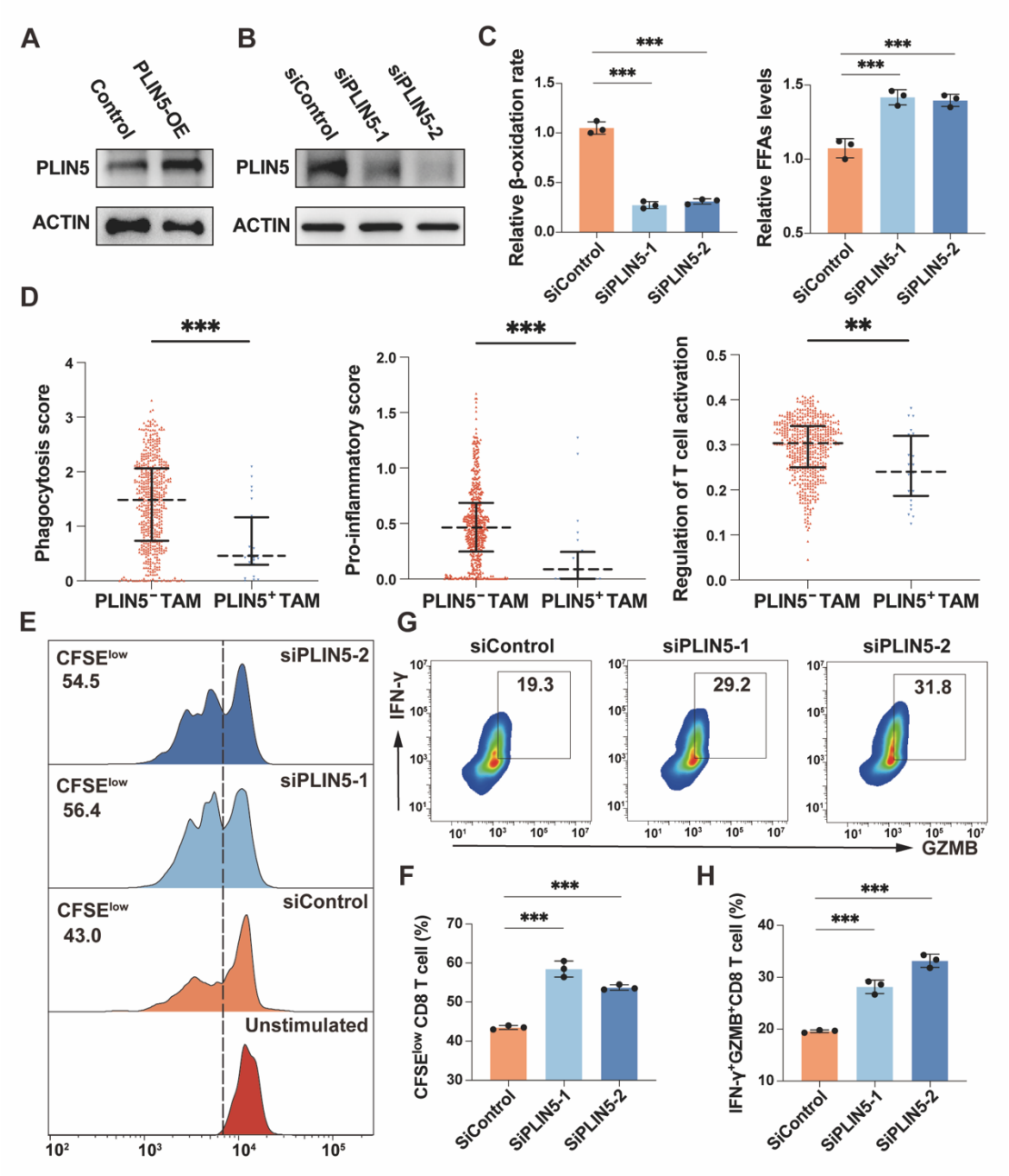

Fig. S11. PLIN5 modulates the immunostimulatory function of TAMs. (A) PLIN5 protein levels in TAMs transfected with either control or PLIN5-overexpression plasmids. (B) PLIN5 protein levels in TAMs transfected with either control siRNA or siRNA targeting PLIN5. (C) β-oxidation rate (left panel) and FFA levels (right panel) were measured in TAMs transfected with either control siRNA or siRNA targeting PLIN5. (D) The expression-based scores for phagocytosis, pro-

inflammatory response, and regulation of T-cell activation were calculated in $PLIN5^-$ TAMs and $PLIN5^+$ TAMs using scRNA-seq data from HCC patients (GSE140228). (E-F) T-cell proliferation assay. Splenic $CD8^+$ T-cells were co-cultured with TAMs transfected with either control siRNA or siRNA targeting PLIN5. The percentage of CFSE low population represents the frequencies of proliferating $CD8^+$ T-cells. Representative flow cytometry data (E) and the statistical diagram (F) are shown. (G-H) Analysis of IFN-γ^+ $GZMB^+$ $CD8^+$ T-cells after co-culturing with TAMs transfected with either control siRNA or siRNA targeting PLIN5. Representative flow cytometry data (G) and the statistical diagram (H) are shown. Statistical analysis was performed using the Student's t-test (or the Mann-Whitney U test in D). Data was presented as mean with SD (or median with IQR in D). $^{**}p<0.01$, $^{***}p<0.001$. PLIN5: Perilipin 5; TAM: tumor-associated macrophage; siRNA: small interfering RNA; FFA: free fatty acid; scRNA-seq: single-cell RNA sequencing; CFSE: carboxyfluorescein succinimidyl ester; IFN-γ: interferon-γ; GZMB: granzyme B; OE: overexpression; SD: standard deviation; IQR: interquartile range.

Fig. S12

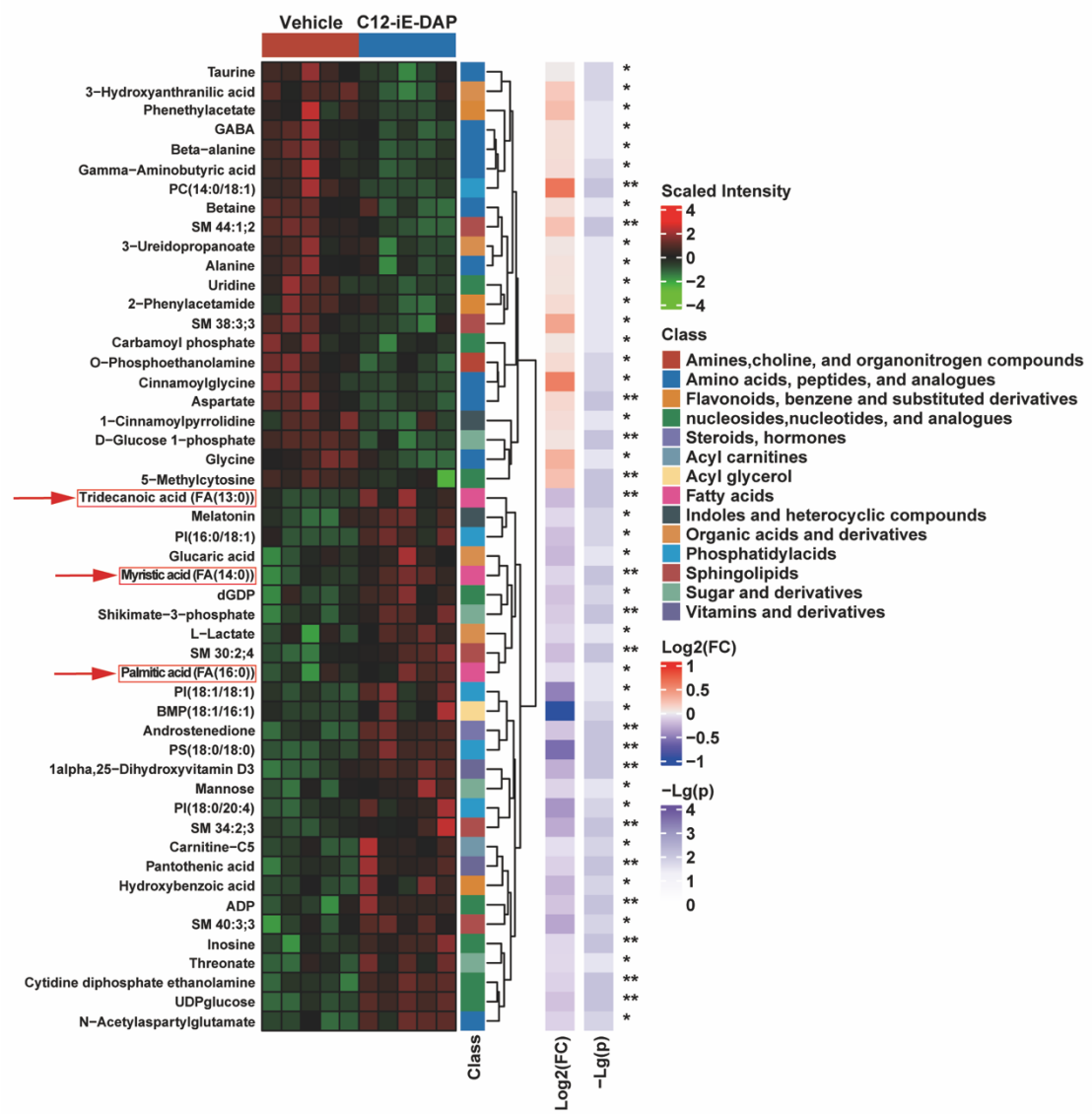

Fig. S12. Hierarchical clustering analysis of differentially expressed metabolites in TAMs treated with either vehicle or C12-iE-DAP. Statistical analysis was performed using the Mann-Whitney U test. *p<0.05, **p<0.01. TAM: tumor-associated macrophage; GABA: γ-aminobutyric acid; PC: phosphatidylcholine; SM: sphingomyelin**;** FA: fatty acid; PI: phosphatidylinositol**;** BMP: bis (monoacylglycero) phosphate; PS: phosphatidylserine**;** FC: fold change.

Fig. S13

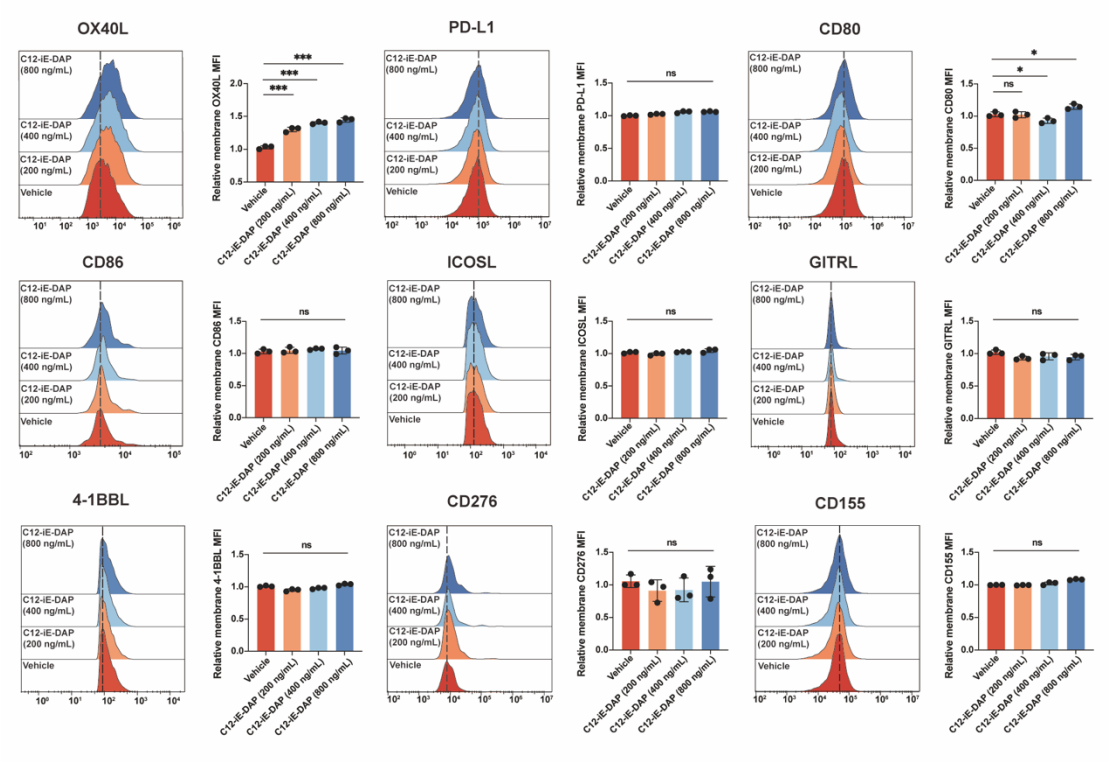

Fig. S13. Flow cytometric analysis of ligands with co-stimulatory or inhibitory activities on TAMs treated with either vehicle or C12-iE-DAP. Statistical analysis was performed using the Student's t-test. Data was presented as mean with SD. ns, no significance; *p<0.05, ***p<0.001. TAM: tumor-associated macrophage; SD: standard deviation.

Fig. S14

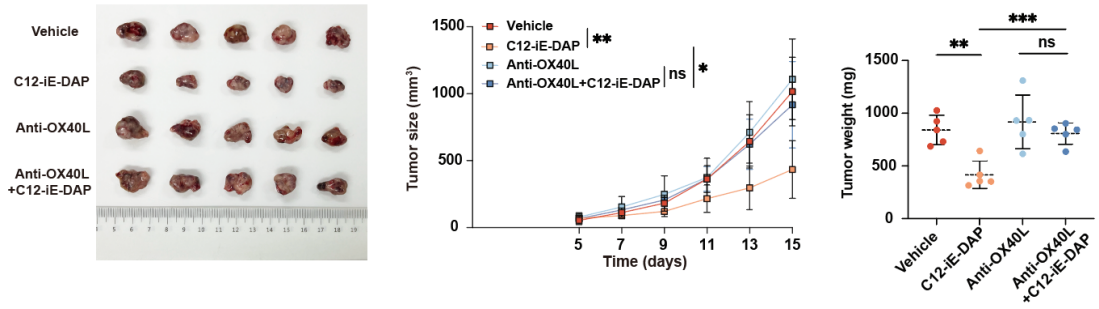

Fig. S14. Tumor growth curves and tumor weights of HCC tumors treated intraperitoneally with either vehicle or C12-iE-DAP (25 μg/injection) in control or OX40L blockade C57BL/6 mice (n=5, each). Statistical analysis was performed using the Student's t-test. Data was presented as mean with SD. ns, no significance; *p<0.05, **p<0.01, ***p<0.001. HCC: hepatocellular carcinoma.

Fig. S15

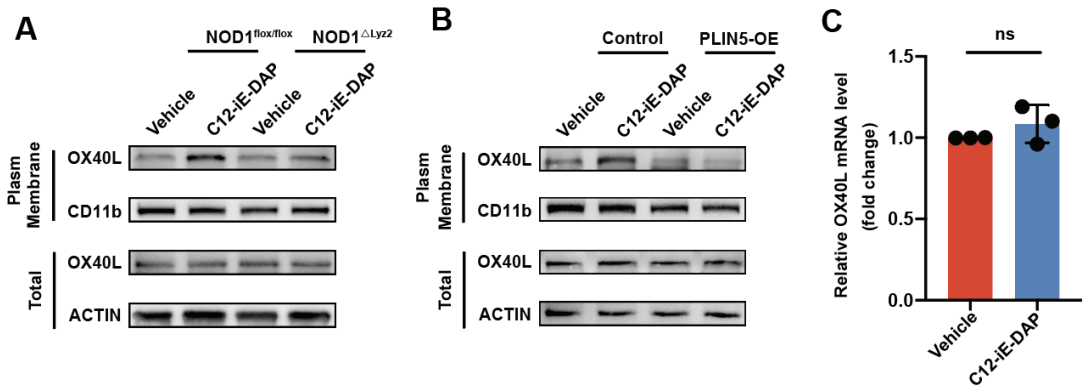

Fig. S15. NOD1 activation promotes OX40L membrane expression in TAMs. (A) Western blot analysis of total OX40L and membrane OX40L expression on TAMs generated from NOD1$^{flox/flox}$ or NOD1$^{\Delta Lyz2}$ mice and treated with either vehicle or C12-iE-DAP. β-actin and CD11b were used as loading controls. (B) Western blot analysis of total OX40L and membrane OX40L expression on TAMs transfected with either control or PLIN5-overexpression plasmids, followed by treatment with either vehicle or C12-iE-DAP. β-actin and CD11b were used as loading controls. (C) qPCR analysis of the mRNA levels of OX40L in TAMs treated with either vehicle or C12-iE-DAP. Statistical analysis was performed using the Student's t-test. Data was presented as mean with SD. ns, no significance. TAM: tumor-associated macrophage; PLIN5: perilipin 5; OE: overexpression; SD: standard deviation.

Fig. S16

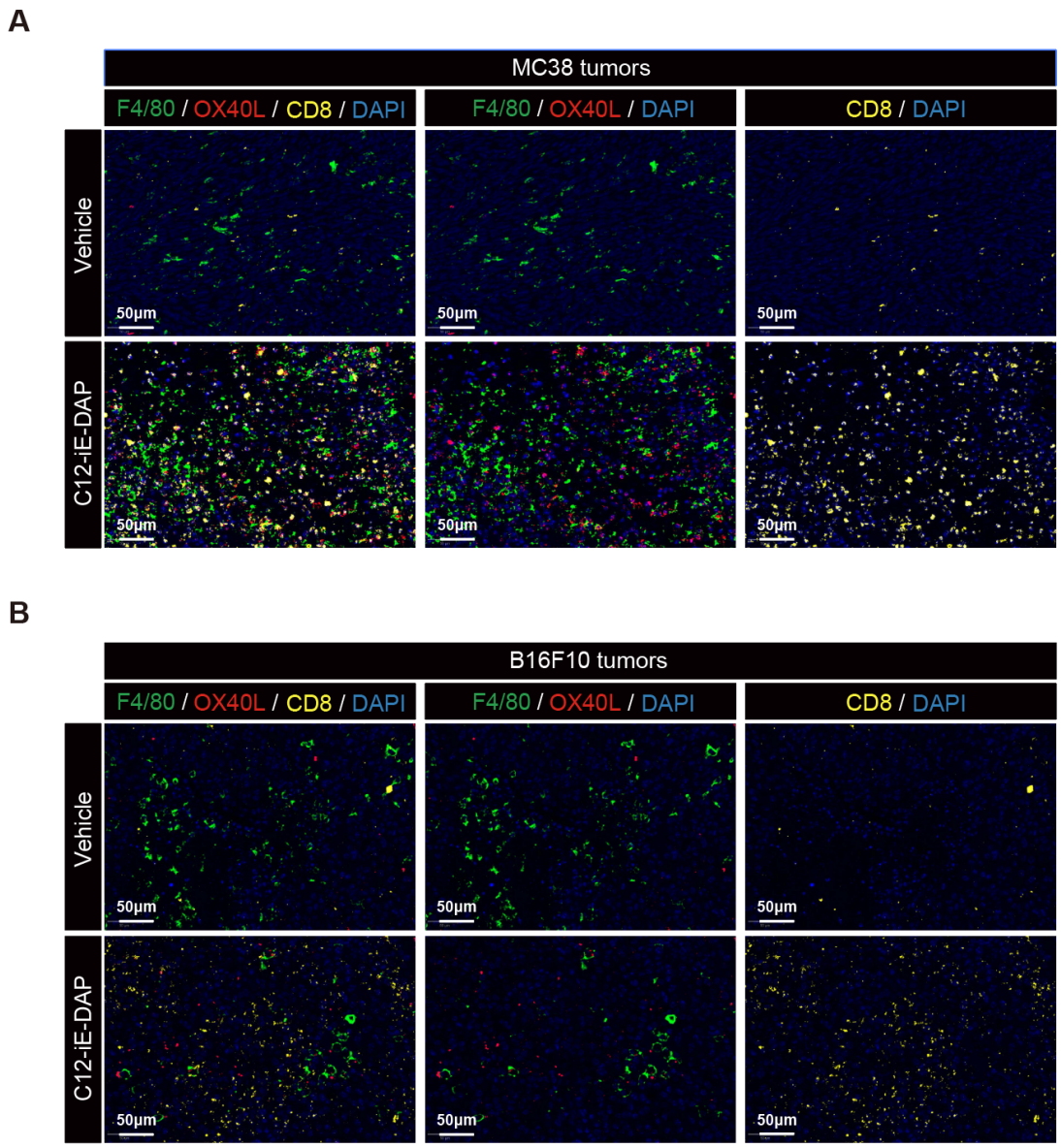

Fig. S16. mIF analysis of OX40L$^+$ TAMs and CD8$^+$ T cells in B16F10 melanoma and MC38 colon carcinoma treated with either vehicle or C12-iE-DAP. (A) Representative pictures of mIF analysis for F4/80, OX40L, and CD8 markers in the MC38 tumors treated with either vehicle or C12-iE-DAP. Scale bar: 50 μm. (B) Representative pictures of mIF analysis for F4/80, OX40L, and CD8 markers in the B16F10 tumors treated with either vehicle or C12-iE-DAP. Scale bar: 50 μm. mIF: multiplex immunofluorescence; TAM: tumor-associated macrophage.

Fig. S17

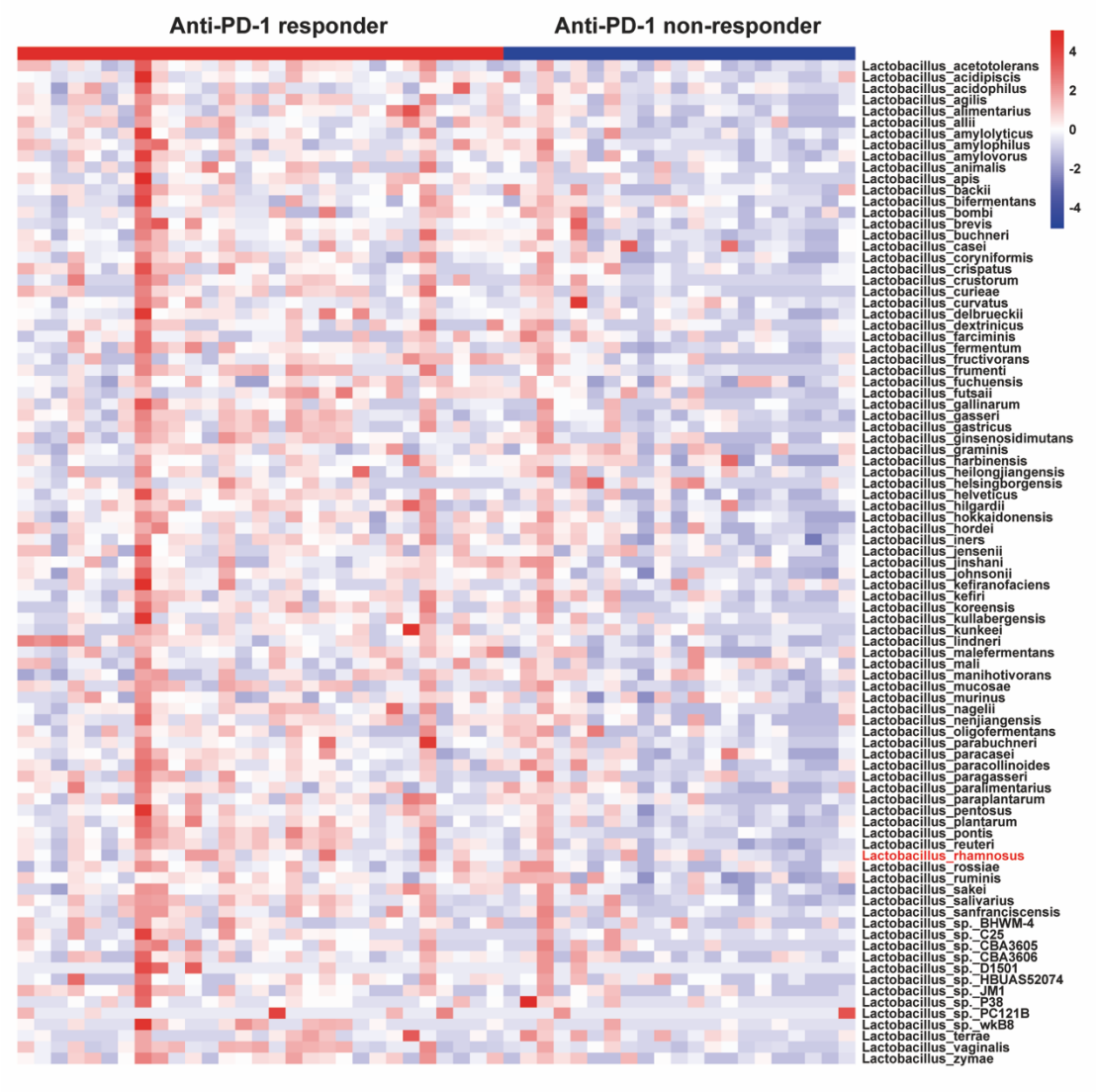

Fig. S17. Heatmap depicting the relative abundance of iE-DAP-bearing *Lactobacillus* between fecal samples from anti-PD-1 responding (n=29) and non-responding (n=21) HCC patients. The color gradient represents the normalized Z scores of each gene across samples, ranging from low (blue) to high (red). *Lactobacillus rhamnosus* GG is highlighted in red.

Fig. S18

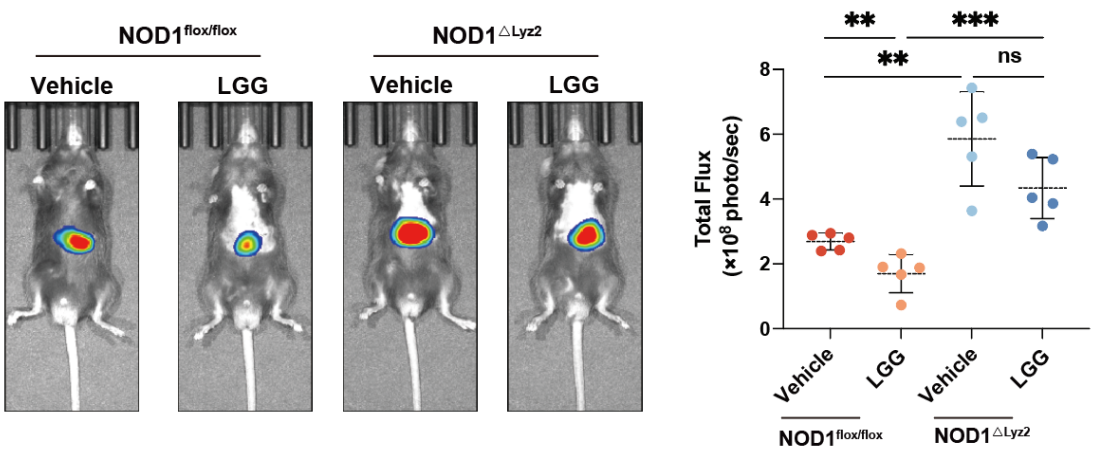

Fig. S18. Orthotopic HCC tumors growing in NOD1$^{flox/flox}$ versus NOD1$^{\Delta Lyz2}$ mice administrated orally with either PBS or LGG (n=5 each). Statistical analysis was performed using the Student's t-test. Data was presented as mean with SD. ns, no significance; **p<0.01; ***p<0.001. HCC: hepatocellular carcinoma; LGG: Lactobacillus rhamnosus GG; SD: standard deviation.

Table S1. Antibodies used for flow cytometry.

Antibody	Clone	Company
anti-human CD45	HI30	eBioscience
anti-human CD11b	M1/70	BD
anti-human CD68	Y1/82A	BioLegend
anti-human NOD1	3F10	US Biological
anti-human CD3	SK7	BD
anti-human CD4	RPA-T4	eBioscience
anti-human CD8	RPA-T8	eBioscience
anti-human CD25	BC96	eBioscience
anti-human CD127	HIL-7R-M21	BD
anti-human CD19	SJ25C1	BioLegend
anti-human CD56	B159	BD
anti-human Ki-67	SolA15	eBioscience
anti-human Perforin	dG9	BioLegend
anti-human Granzyme B	GB11	BioLegend
anti-human PD-1	NAT105	BioLegend
anti-human CTLA-4	14D3	eBioscience
anti-human TIGIT	741182	BD
anti-mouse CD45	30-F11	BD
anti-mouse CD3	145-2C11	BioLegend
anti-mouse CD8	53-6.7	BioLegend
anti-mouse IFN-γ	XMG1.2	BioLegend
anti-mouse Granzyme B	NGZB	eBioscience
anti-mouse PD-1	29F.1A12	BioLegend
anti-mouse CD11b	M1/70	BioLegend
anti-mouse F4/80	T45-2342	BD
anti-mouse CD206	C068C2	BioLegend
anti-mouse MHC-II	M5/114.15.2	eBioscience
anti-mouse OX40L	RM134L	BioLegend
anti-mouse PD-L1	MIH5	eBioscience
anti-mouse CD80	16-10A1	BioLegend
anti-mouse CD86	GL-1	BioLegend
anti-mouse ICOSL	HK5.3	BioLegend
anti-mouse GITRL	YGL386	BioLegend
anti-mouse 4-1BBL	TKS-1	BioLegend
anti-mouse B7-H3	MIH35	BioLegend
anti-mouse CD155	TX56	BioLegend

Table S2. Primers used for quantitative real-time PCR in this study.

Name	Forward Sequence (5' to 3')	Reverse Sequence (3' to 5')
β-actin	GGCTGTATTCCCCTCCATCG	CCAGTTGGTAACAATGCCATGT
Arg	CTCCAAGCCAAAGTCCTTAGAG	AGGAGCTGTCATTAGGGACATC
Fizz	CCAATCCAGCTAACTATCCCTCC	ACCCAGTAGCAGTCATCCCA
Il10	GCTCTTACTGACTGGCATGAG	CGCAGCTCTAGGAGCATGTG
Mrc1	CTCTGTTCAGCTATTGGACGC	CGGAATTTCTGGGATTCAGCTTC
Il1b	GCAACTGTTCCTGAACTCAACT	ATCTTTTGGGGTCCGTCAACT
Il6	TAGTCCTTCCTACCCCAATTTCC	TTGGTCCTTAGCCACTCCTTC
Il12b	TGGTTTGCCATCGTTTTGCTG	ACAGGTGAGGTTCACTGTTTCT
Tnfα	CCCTCACACTCAGATCATCTTCT	GCTACGACGTGGGCTACAG
Ccl12	ATTTCCACACTTCTATGCCTCCT	ATCCAGTATGGTCCTGAAGATCA
Ccl8	TCTACGCAGTGCTTCTTTGCC	AAGGGGGATCTTCAGCTTTAGTA
Cxcl2	CCAACCACCAGGCTACAGG	GCGTCACACTCAAGCTCTG
Icam1	GTGATGCTCAGGTATCCATCCA	CACAGTTCTCAAAGCACAGCG
Ido1	GCTTTGCTCTACCACATCCAC	CAGGCGCTGTAACCTGTGT
Fasn	GGAGGTGGTGATAGCCGGTAT	TGGGTAATCCATAGAGCCCAG
Acss2	AAACACGCTCAGGGAAAATCA	ACCGTAGATGTATCCCCCAGG
Acsl4	CTCACCATTATATTGCTGCCTGT	TCTCTTTGCCATAGCGTTTTTCT
Scd1	TTCTTGCGATACACTCTGGTGC	CGGGATTGAATGTTCTTGTCGT
Scap	TGGAGCTTTTGAGACTCAGGA	TCGATTAAGCAGGTGAGGTCG
Acaca	GATGAACCATCTCCGTTGGC	GACCCAATTATGAATCGGGAGTG
Dgat1	TCCGTCCAGGGTGGTAGTG	TGAACAAAGAATCTTGCAGACGA
Hadha	TGCATTTGCCGCAGCTTTAC	GTTGGCCCAGATTTCGTTCA
Cpt1a	CTCCGCCTGAGCCATGAAG	CACCAGTGATGATGCCATTCT
Ppara	AGAGCCCCATCTGTCCTCTC	ACTGGTAGTCTGCAAAACCAAA
Srebf1	TGACCCGGCTATTCCGTGA	CTGGGCTGAGCAATACAGTTC
Cd36	ATGGGCTGTGATCGGAACTG	TTTGCCACGTCATCTGGGTTT
Ldlr	TGACTCAGACGAACAAGGCTG	ATCTAGGCAATCTCGGTCTCC
Mgll	CGGACTTCCAAGTTTTTGTCAGA	GCAGCCACTAGGATGGAGATG
Atgl	GGATGGCGGCATTTCAGACA	CAAAGGGTTGGGTTGGTTCAG
Hsl	CCAGCCTGAGGGCTTACTG	CTCCATTGACTGTGACATCTCG
Lpl	GGGAGTTTGGCTCCAGAGTTT	TGTGTCTTCAGGGGTCCTTAG
Plin1	GGGACCTGTGAGTGCTTCC	GTATTGAAGAGCCGGGATCTTTT
Plin2	GACCTTGTGTCCTCCGCTTAT	CAACCGCAATTTGTGGCTC
Plin3	ATGTCTAGCAATGGTACAGATGC	CGTGGAACTGATAAGAGGCAGG
Plin4	GTGTCCACCAACTCACAGATG	GGACCATTCCTTTTGCAGCAT
Plin5	TGTCCAGTGCTTACAACTCGG	CAGGGCACAGGTAGTCACAC
Ox40l	AATCTGGAAAACGGATCAAGGC	CAGGCAGACATAGATGAAGCAC